Analysis of anisotropic prismatic sections

G. F. J. Hill and P. M. Weaver
Department of Aerospace Engineering, University of Bristol
Bristol, UK

ABSTRACT

The dynamic behaviour of rotor blades is often modelled using one-dimensional beam analysis with equivalent mass and stiffness properties to those of the full blade. Calculation of accurate elastic stiffness terms for these arbitrarily shaped sections with differing material properties is vital to this process. A method which produces these properties using standard finite element analysis codes is presented. The method is then compared with theoretical results for a simple rectangular section beam and case studies are performed on a composite laminate and box-section.

NOMENCLATURE

a,b,c	unknown coefficients in Equation (8)
	material elastic modulus
F	force
G	material shear modulus
I	second moment of area
J	polar moment of area
k	shear constant
$\mathbf{K}$	stiffness matrix terms
M	moment
P	independent nodes (first face)
Q	dependent nodes (second face)
r	rotational degrees of freedom about x,y,z
R_{My}	axial reaction force at constraints due to load case M_y
R_{Mz}	axial reaction force at constraints due to load case M_z
$\mathbf{S}$	flexibility matrix terms
u,v,w	translational degrees of freedom in x,y,z, respectively
x,y,z	global co-ordinates relative to the origin
μ_i	beam translational scalar freedoms
ν	material Poisson ratio
ω	beam rotational scalar freedoms

1.0 INTRODUCTION

From a modelling perspective, one of the most complicated closed-section beam-type structures of practical importance is a helicopter rotor blade. Helicopter rotor blades are complex in both construction and structural response. Typically they may be 6-10m in length with chord lengths and depths approximately 600mm and 100mm, respectively. Furthermore, since the 1970s they have been constructed from highly anisotropic composite materials (carbon fibre/epoxy, Rohacell foam and Nomex honeycomb). Structurally, they may be considered as slender one-dimensional elements subject to extensional (centrifugal), torsional and bi-directional bending loads. Their behavioural response can be further complicated by intrinsic coupling between

- centrifugal loads and twisting
- torsional loads and extension
- flexural loads and twisting
- torsional moment and flexure,

due to the non-coincidence of shear, flexural and mass centres that stems from the asymmetric nature of the cross-section and material

Paper No. 2845. Manuscript received 5 June 2003, revised version received 30 January 2004, accepted 2 March 2004.

https://doi.org/10.1017/S0001924000000105 Published online by Cambridge University Press

composition. Indeed, the latter type of coupling has been the centre of much attention since Mansfield and Sobey raised the possibility of aeroelastic coupling on tailoring dynamic performance[1]. The problem, as it stands, is too complex to solve analytically and is beyond the processing power of present-day computers. Rough calculations show that if the entire rotor blade was constructed from cubic 3D finite elements the size of the resulting stiffness matrix would be of the order of tens of Terabytes! Herein, lies the crux of the problem, to apply appropriate modelling techiques to simplify the problem to current processing power levels whilst at the same time retaining the most important physical characteristics. It is the calculation of the cross-sectional stiffness parameters which becomes the main issue in performing accurate analyses of rotor blade designs. The assessment of these properties has been investigated widely with isotropic sections. Many sections have exact analytical solutions for many of the properties required, including the definition of the elastic and shear centres[2].

The development of a method which can calculate the equivalent 1D beam properties for arbitrary sections composed of non-homogeneous anisotropic materials is desired by industry. In addition to helicopter rotor blades there are other examples in the aerospace industry where there is a need to model arbitrary shaped tubes accurately. These include propellers and main spars such as those found in the Westland Lynx tailplane. There are modelling opportunities outside of the Aerospace industry too. Sporting equipment such as golf club shafts, tennis rackets and ski-poles as well as offshore platform structures are to name but a selected few examples where closed section composite tubes are subjected to various loads. Potentially, there is scope for optimising the composite lay-up and taper of such structures. The overall aim of the paper is to develop an analysis for calculating the 6×6 stiffness matrix of beams. An equally important objective is to formulate the analysis so that it can be readily implemented into standard software, a requirement that is particularly sought by industry. In the opening section a review of cross-section property calculation methods and their effectiveness based on assumptions made in their formulation is made. One of these methods is extended to include the calculation of equivalent beam shear stiffness, giving a full 6×6 stiffness matrix. Finally, examples are given to show the effectiveness of the method in predicting stiffness terms and equivalent dynamic behaviour of the beams.

2.0 BACKGROUND

Most of the work on analysis of one-dimensional hollow composite closed sections has concerned helicopter rotor blades. Pioneering work was undertaken by Mansfield and Sobey[1], Mansfield[3] and later by Bartholomew and Mercer[4]. Of particular merit is the work of Bartholomew and Mercer[4] who simplify the 3D complexity by reducing the problem to a thin slice analysis of a unit-length cross-section of blade. By postulating a displacement field that includes extensional, flexural, twisting and warping effects, they use commercial finite element (FE) analysis to establish shear and flexural centres. As such, flexural stiffness, extension stiffness and twisting stiffness are defined that may be used in subsequent 1D beam analysis of the rotor blade. Complete anisotropic behaviour is represented in the model. The chief assumption is that stresses are at most a linear function of the length coordinate, which is reasonable for beams whose material and geometric properties vary slowly with length. This technique is relatively straightforward to implement and directly generates beam data that may be used in a subsequent one-dimensional beam analysis. However, it does not include the effects of restrained warping or shear deformation effects.

Early, yet notable work by wörndle[5] calculated magnitudes of various warpings for a rotor blade section. This model may be viewed as a special case of that of Bartholomew and Mercer. Although Wörndle included some anisotropic behaviour the most important type of extension/twist and flexural/twist is omitted due the assumption of orthotropy along the blade. Furthermore, wörndle concentrates on the application of a shear load and response and does not examine flexural response. Also, through-thickness stresses are ignored in this work.

Giavotto[6] presents a complex 2D finite element based approach that models complete anisotropy in addition to restrained warping effects. Kosmatka's approach[7-10], although similar to that of Bartholomew and Mercer's earlier work, relies on identification of shear and flexural centres that characterise direct responses. His displacement functions are identical with that of Bartholomew and Mercer, both having been derived using an approach previously suggested by Lekhnitskii[11]. His numerical model, including effects of anisotropic behaviour and warping, leads to various stiffness terms that can be used in a one-dimensional beam element model. Structural responses in terms of shear, warping, extension and flexure are averaged over the cross-section. Through thickness stresses are included in all cases. Like Bartholomew and Mercer's earlier model, arbitrary sectional shapes can be modelled. Kosmatka's work advances Bartholomew and Mercer's work in a number of ways. The effect of shear loading is included, and so can better represent moment/curvature relationships. Furthermore, greater physical insight into the problem is gained since all displacement functions (including warping) are evaluated. Kosmatka, because of this detail, shows that in-plane warping must be considered in addition to out-of-plane warping in the analysis of anisotropic sections. The drawback with Kosmatka's method is one of complexity and difficulty of implementation.

Many other workers have modelled helicopter rotor blades. Hodges[12] summarised the modelling approaches into those that were analytical and those that were finite element based. Recent analytical methods[13,14] can model discontinuous material behaviour but rely on thin-walled assumptions. Recent work by Hodges and co-workers[15,16] employ a 2D FE approach to calculate stiffness properties and couple this with subsequent 1D beam analysis[23,24].

Recently, Rand and co-workers at the Israel Institute of Technology have been prolific in their output on rotor blade analysis[17-20]. While offering closed form solutions, for example on rectangular sectioned composite beams, and emphasising the link between in- and out-of-plane warping due to material couplings on flexural response, the model of warping is similar to that of Kosmatka. Other authors have tackled the problem by formulating beam models for box-sections in a one-step analysis[21,22]. Of particular note is the work of Chandra *et al* who validate their model with experimental results[23,24].

The simplicity of Bartholomew and Mercer's method and its use of standard finite element analysis codes make it ideal to analyse cross-section properties. Its chief limitation, however, is its omission of shear loading and deformation, and was advanced recently by the current authors[25,26]. The present paper extends this work further to include validation case studies and dynamic beam analysis.

The currently reported method has been automated using a combination of PATRAN command language (PCL) within MSC/PATRAN[27] to create the models and MSC/NASTRAN[28] for analysis. It is known as NASSAN (NAStran Structural ANalysis). It is, of course, possible to encode the method with any suitable finite element analysis package.

3.0 BARTHOLOMEW AND MERCER'S METHOD

Bartholomew and Mercer[4] use the beam model as defined by Lekhnitskii[11] and simplified the analysis by considering the relative displacement and rotation between any point P1 on section x_1 (face P) at position (y,z) and the corresponding point, Q1 of the same position (y,z), at a section x_2 (face Q). Evaluating the difference in displacements and rotations on opposite faces of a finite section, as

https://doi.org/10.1017/S0001924000000105 Published online by Cambridge University Press

shown in the three dimensional beam slice in Fig. 1, eliminates the consideration of deformation components that are independent of length, such as in-plane warping. As such the relationships between relative displacements and rotations are obtained as;

$$u(Q)-u(P)=\mu_x+\omega_y z-\omega_z y \quad \ldots (1)$$

$$v(Q)-v(P)=\mu_y-\omega_x z \quad \ldots (2)$$

$$w(Q)-w(P)=\mu_z+\omega_x y \quad \ldots (3)$$

$$r_x(Q)-r_x(P)=\omega_x \quad \ldots (4)$$

$$r_y(Q)-r_y(P)=\omega_y \quad \ldots (5)$$

$$r_z(Q)-r_z(P)=\omega_z \quad \ldots (6)$$

where $\mu_y=\mu_z=0$ to stop rigid body rotation.

Bartholomew and Mercer implemented these expressions into finite element analysis through the use of multi-point constraint equations (MPCs). As such, the deformations of face P must follow those of face Q and indeed obey the relations given in Equations (1) – (6). Furthermore, each of the nodes on face Q must deform uniformly in the sense that the displacements (μ_i) and the rotations (ω_i) are identical. This constraint is included in the same MPCs indicated above by introducing degrees of freedom (scalar freedoms) into the model that control the deformation response of face Q. In general, the scalar freedoms are introduced at an extra node. This node is linked to all nodes on face Q through the set of MPCs.

An important feature of the model is that there is no restriction on deformation response within a section and as such represents 2D continuum response as accurately as the mesh density allows. The MPCs simply reduce the number of longitudinal degrees of freedom to that of a one-dimensional beam model. To calculate standard (and non-standard) beam properties such as axial stiffness, *EA*, or flexural stiffness, *EI* it is a simple matter of applying the appropriate force (or bending moment) to the scalar freedom and measure the resultant displacement or rotation (μ and ω). Since the model is of unit length these displacements and rotations also represent strains and curvatures. As such, from now on, the same notation is used to represent both, the nature of which is apparent from the context.

The first stage of the analysis is to apply unit loads to the four active scalar freedoms which evenly distribute the loads to all the elements in the model. The load cases are axial tension, torsion about the *x*-axis and bending about the *y* and *z*-axes. The two shear force directions cannot be loaded directly as part of this analysis as they have been restrained to stop rigid body rotations.

For each load case, the four active scalar freedoms provide the overall displacements in the degree of freedom which they represent. Therefore, the axial displacement and the three rotational displacements are available. The flexibilities (***S***), equivalent to strains and curvatures of the section (Equation (7)) are found by dividing these displacements by the original length of the slice model, usually unity. This gives the derivative terms being calculated as;

$$\begin{Bmatrix}\mu_x\\ \omega_x\\ \omega_y\\ \omega_z\end{Bmatrix}=\begin{pmatrix}S_{11} & S_{14} & S_{15} & S_{16}\\ S_{41} & S_{44} & S_{45} & S_{46}\\ S_{51} & S_{54} & S_{55} & S_{56}\\ S_{61} & S_{64} & S_{65} & S_{66}\end{pmatrix}\begin{Bmatrix}F_x\\ M_x\\ M_y\\ M_z\end{Bmatrix} \quad \ldots (7)$$

as shown previously by Bartholomew and Mercer[4].

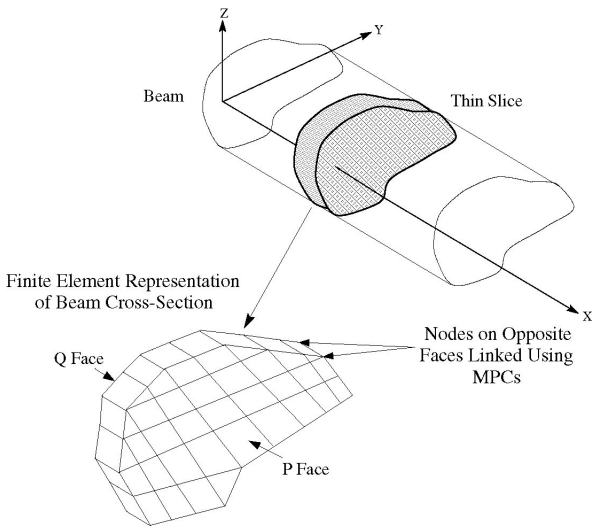


Figure 1. Representation of mesh for Bartholomew and Mercer's method.

This flexibility matrix is only 4 × 4 in nature, and does not include any shear loading or shear flexibilities. The shear flexibilities are not available directly from the scalar freedoms because they are set to zero. It is possible, however, to calculate them from any out-of-plane deformations due to the four load cases applied so far. This is akin to the approach used by Timoshenko[29] to evaluate shear coefficients in slender beams. In this case, however, we are dealing with shear deformations in both the *y* and *z* directions simultaneously.

The method described applies to any prismatic section of infinite length. In theory, warping stresses that arise at a fixed end may develop that decay very quickly for a closed section and less so for an open section. In practice, the effects of these are expected to be minimal for a closed section since the fixed end is generally reinforced to a fair degree. For open sections, warping stresses decay over much greater length scales such that longitudinal stresses may be in excess of that predicted in the method shown here, some distance away from a loading or fixed point.

3.1 Calculating the shear flexibility of the section

For each load case so far applied, all the nodes on each face will have displaced in the axial, *x*, direction. If shear displacement has taken place due to either torque (M_x) applied away from the shear centre or material coupling, then there will be a mean slope to the displacements of both faces. Evaluation of the average slopes gives estimates of the shear flexibilities of the cross-section.

The procedure involves post-processing the *x*-displacements of all the nodes in the section according to the following method. A suitable equation of a plane in 3D space is

$$x=a+by+cz \quad \ldots (8)$$

and from the FE analysis, each node pairing will have a mean axial displacement

$$\delta x=\frac{\delta x^P+\delta x^Q}{2} \quad \ldots (9)$$

with the error between Equations (8) and (9) given by

$$Error=a+by+cz-\delta x \quad \ldots (10)$$

This error is minimised using a least squares approach,

$$Error^2=(a+by+cz-\delta x)^2 \quad \ldots (11)$$

https://doi.org/10.1017/S0001924000000105 Published online by Cambridge University Press

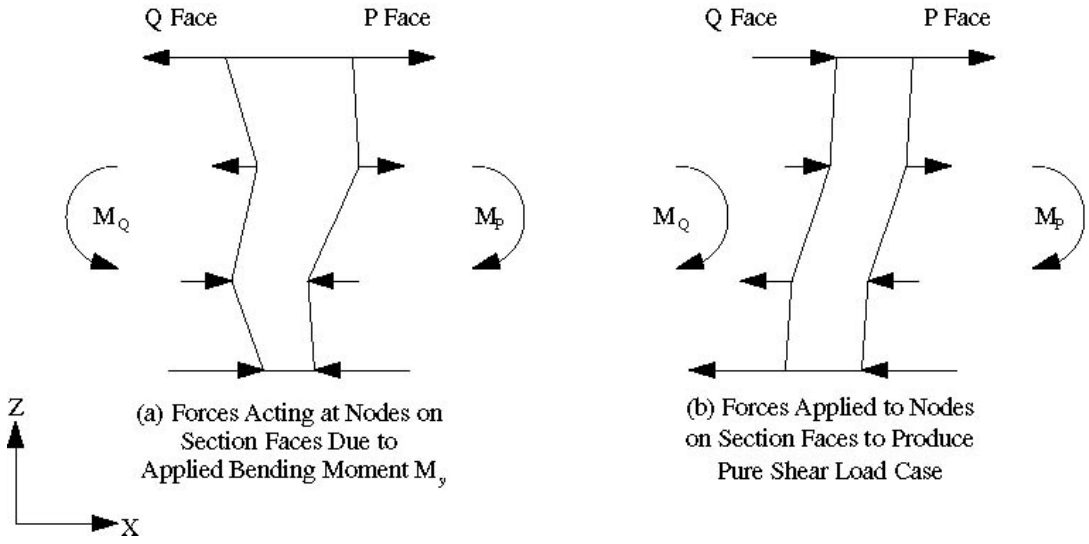


Figure 2. Schematic of load case for pure shear.

As the error is a function of a, b and c, to minimise it is necessary to differentiate with respect to a, b and c during the process of summation of all node pair results, as follows;

$$\sum \frac{\delta Error}{\delta a} = \sum 2(a + by + cz - \delta x) = 0 \quad \ldots (12)$$

$$\sum \frac{\delta Error}{\delta b} = \sum 2y(a + by + cz - \delta x) = 0 \quad \ldots (13)$$

$$\sum \frac{\delta Error}{\delta c} = \sum 2z(a + by + cz - \delta x) = 0 \quad \ldots (14)$$

The simplest way to solve these equations and evaluate the slopes of the least squares fit surface, and hence the flexibility terms, is to use a matrix method. The slopes of the surface (b and c) are the shear flexibilities in the y and z directions respectively. It is important to distribute the nodes throughout the section evenly because node clustering can cause biased results.

The shear flexibilities need to be calculated for every applied load case to fill the missing terms from the flexibility matrix. For example, for the axial force (F_x) case,

$$S_{12} = b \quad \ldots (15)$$

$$S_{13} = c \quad \ldots (16)$$

and similarly for the other load cases.

3.2 Applying the shear load cases

The scalar freedoms for y and z shear cannot be loaded directly in shear because the section needs to be restrained to stop rigid body rotations. Following Bartholomew and Mercer[4] it is possible, however, to load the nodes of independent face P axially to simulate the transverse shear loading.

Figure 2(a) shows a uniform bending moment acting on a section of unit length and the longitudinal forces that arise to maintain static equilibrium. By extracting the magnitude of longitudinal forces at each node on a face gives an indirect method for introducing pure shear to the model. Pure shear may be obtained by reversing the direction of axial forces on the P face, as shown in Fig. 2(b). This is readily justified in terms of simple beam analysis. By expressing shear force, F, as the rate of change of bending moment, it is obvious that the scenario in Fig. 2(a) has zero shear force since

$$F = \frac{M_P - M_Q}{1} \quad \ldots (17)$$

equals zero since $M_P = M_Q$. However the shear force in Fig. 2(b) is given by $2M_y$ since in this case, $M_Q = -M_P$ with $M_P = M_Q$. Note the total bending moment in Fig. 2(b) is zero and as such represents a state of pure shear. It is noted that the vertical edges of sections do not necessarily remain straight and depend on the nature of elastic material properties through the section. For example, the piecewise linear distribution shown in Fig. 2.

The forces necessary to do this can be taken directly from the bending load cases performed in the first analysis run. The force reactions on the nodes of face P as a result of the MPC equations applied to the same nodes. The nodes on face Q do not need to be loaded as the axial degrees of freedom have already been eliminated by the MPCs. The magnitudes of the axial forces on the nodes of face P need to be halved to achieve a unit shear load. The axial forces applied at each node on face P for the shear load F_z are taken from the M_y load case

$$F_x = \frac{-R_{M_y}}{2} \quad \ldots (18)$$

and similarly for the F_y case taken from the results from M_z,

$$F_x = \frac{R_{M_z}}{2} \quad \ldots (19)$$

where the direction is not reversed as the sense of the forces on the nodes is correct for a positive shear force.

These additional shear load analyses are run and the four free scalar freedoms (μ_1 and ω_1, ω_2, ω_3) used directly as the flexibilities for the two shear cases. The shear flexibilities need to be calculated from the slopes of the faces as shown previously.

At this point, a full 6×6 flexibility matrix has been calculated,

https://doi.org/10.1017/S0001924000000105 Published online by Cambridge University Press

coupling all six degrees of freedom with one another. This matrix should be symmetric about the leading diagonal, providing the finite element mesh is refined enough for the given problem. If the significant 'symmetric' terms are not within 5% of each other then it is probably necessary to re-analyse the section with a more refined mesh, especially in regions of sudden change in properties.

3.3 Elastic and shear centres

The location of the elastic centroid with respect to the beam neutral axes (y_{ec}, z_{ec}) is found by considering the amount of bending due to axial tension compared with the amount of bending caused by applying a unit moment. It is therefore located using

$$y_{ec} = \frac{S_{61}}{S_{66}} \quad \ldots (20)$$

$$z_{ec} = -\frac{S_{51}}{S_{55}} \quad \ldots (21)$$

If the shear centre of the section is not on the x-axis ($y = z = 0$), then loading in shear can produce a torque about the x-axis as well as the overall shear force at the restrained scalar freedom in the loaded direction. This reacted force at the scalar freedom will be distributed across the section of the model according to relative stiffness of each element.

The shear centres are calculated from the results of the two load cases using,

$$y_{sc} = -\frac{S_{43}}{S_{44}} \quad \ldots (22)$$

$$z_{sc} = \frac{S_{42}}{S_{44}} \quad \ldots (23)$$

where the two and three subscripts refer to loading in the Y and Z directions, respectively.

3.4 Transformations

The location of the elastic centre can then be used to transform the flexibility properties **S** of the beam to the elastic centroid, the default setting for 1D beam elements in FE. The transformation matrix to translate the beam properties is

$$\mathbf{R} = \begin{pmatrix} 1 & 0 & 0 & 0 & 0 & 0 \\ 0 & 1 & 0 & 0 & 0 & 0 \\ 0 & 0 & 1 & 0 & 0 & 0 \\ 0 & -z_{ec} & y_{ec} & 1 & 0 & 0 \\ z_{ec} & 0 & 0 & 0 & 1 & 0 \\ -y_{ec} & 0 & 0 & 0 & 0 & 1 \end{pmatrix} \quad \ldots (24)$$

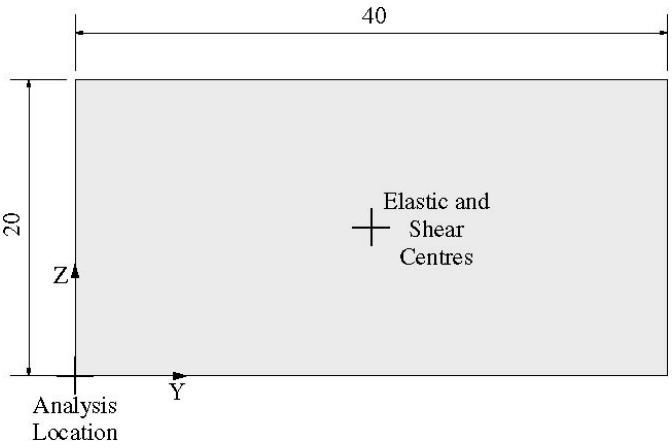


Figure 3. 40 x 20 isotropic rectangular section.

and the transformed matrix [$\bar{S}$] follows as:

$$\bar{\mathbf{S}} = \mathbf{R}^T\mathbf{S}\mathbf{R} \quad \ldots (25)$$

It is, of course, possible to transform flexibilities to any location in the plane of the cross-section, if required. The equivalent stiffness terms (**K**) are found by inverting the flexibility matrix using, for example, Gauss-Jordan methods.

4.0 EXAMPLES

4.1 Isotropic rectangular beam 40 × 20mm

The first example is an isotropic rectangular beam section with co-ordinates at the bottom left hand corner as shown in Fig. 3. This was done to introduce coupling terms in the results and to test the transformation matrix. The mesh consisted of one element for each mm of the cross-section, so was therefore 40 × 20 elements. The material used was a generic aluminium alloy, with a Young's modulus of 70GPa and Poisson's ratio of 0·3.

As the 'Analysis Location' was not at the same position as the elastic and shear centres of the section, coupling was expected in the results. This coupling behaviour can be seen in the following flexibility matrix featured in Equation (26) where the values are truncated to three decimal places, and the relatively small values, lesser in magnitude than 10^{-13}, have been ignored. These arise due to asymmetries and coarseness of mesh density for the cross-section.

Using Equations (20-23) to calculate the elastic and shear centre locations gave the elastic centre at (20.000, 10.000) and the shear centre at (20·000, 9·999) accurate to three decimal places. These 'as

$$\mathbf{S} = \begin{pmatrix} 1{\cdot}249\times10^{-7} & 0 & 0 & 0 & -5{\cdot}357\times10^{-9} & 2{\cdot}678\times10^{-9} \\ 0 & 1{\cdot}057\times10^{-7} & -1{\cdot}014\times10^{-7} & 5{\cdot}070\times10^{-9} & 0 & 0 \\ 0 & -1{\cdot}014\times10^{-7} & 2{\cdot}571\times10^{-7} & -1{\cdot}014\times10^{-8} & 0 & 0 \\ 0 & 5{\cdot}070\times10^{-9} & -1{\cdot}014\times10^{-8} & 5{\cdot}070\times10^{-10} & 0 & 0 \\ -5{\cdot}357\times10^{-9} & 0 & 0 & 0 & 5{\cdot}357\times10^{-10} & 0 \\ 2{\cdot}678\times10^{-9} & 0 & 0 & 0 & 0 & 1{\cdot}339\times10^{-10} \end{pmatrix} \quad \ldots (26)$$

https://doi.org/10.1017/S0001924000000105 Published online by Cambridge University Press

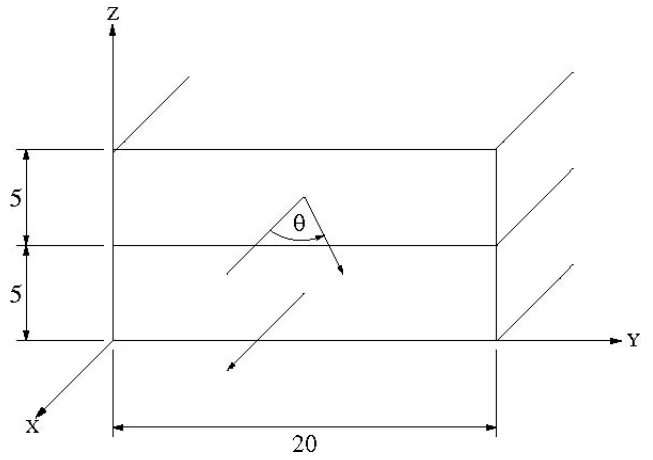


Figure 4. Geometry of anisotropic 20 x 10 block.

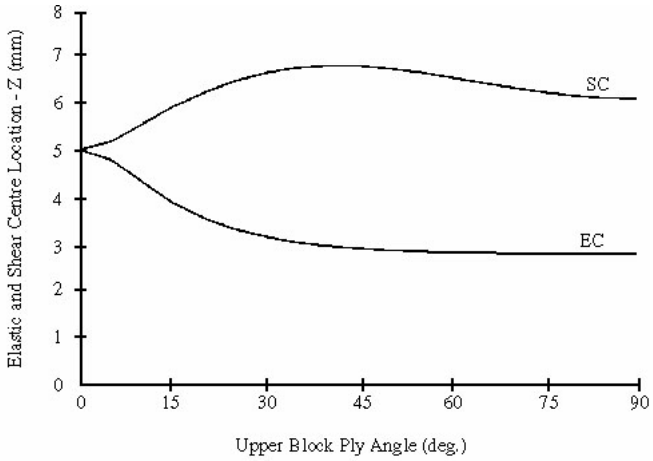


Figure 5. Variation of elastic and shear centres in *Z*-direction.

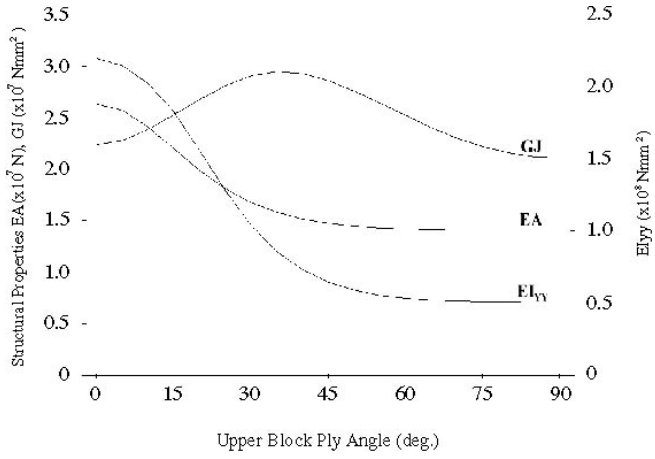


Figure 6. Structural properties for composite rectangular section.

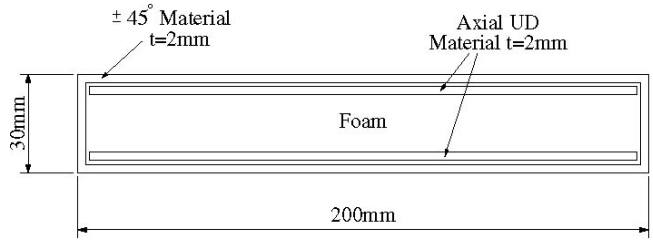


Figure 7. Cross-section of normal mode example.

Table 1
Comparison of beam section stiffness – theory and FE

Property	Theory	FE	Difference
Axial Stiffness N	$5{\cdot}600 \times 10^7$	$5{\cdot}600 \times 10^7$	0·0%
Shear Stiffness (*Y*) N	$1{\cdot}795 \times 10^7$	$1{\cdot}817 \times 10^7$	+1·2%
Shear Coefficient (*Y*)	0·833	0·843	+1·2%
Shear Stiffness (*Z*) N	$1{\cdot}795 \times 10^7$	$1{\cdot}839 \times 10^7$	+2·4%
Shear Coefficient (*Z*)	0·833	0·853	+2·4%
Torsional Stiffness Nmm^2	$1{\cdot}925 \times 10^9$	$1{\cdot}972 \times 10^9$	+2·4%
Bending Stiffness (*Y*) Nmm^2	$1{\cdot}867 \times 10^9$	$1{\cdot}867 \times 10^9$	0·0%
Bending Stiffness (*Z*) Nmm^2	$7{\cdot}467 \times 10^9$	$7{\cdot}467 \times 10^9$	0·0%

analysed' flexibility values were transformed to the elastic and shear centres at (20·000, 10·000), and are shown in Equation (27) where values of less than order 10^{-13} are once again ignored.

The stiffness matrix for the section was obtained by direct inversion, and are shown in Equation (28). The values can be compared to standard analytical solutions for beam behaviour to establish the accuracy of the method when applied to simple isotropic sections. The analytical values shown in Table 1 for the stiffness properties of sections were taken from Young[2].

The only errors are in the shear and torsional stiffnesses, and are small. The discrepancies are due to mesh density, and can be reduced by increasing the number of elements in each direction as shown in Table 2. The linear displacement function elements being used in this analysis are only capable of constant stress fields, so find it difficult to represent the parabolic stress distributions found in the shear load cases. More elements increase the accuracy of the stress field, and hence the stiffness calculation. It should be noted that even better performance can be gained by using parabolic displacement function elements. The equations used to link the two faces of the slice model do not need to be altered with higher order function elements.

4.2 Property variation with lay-up

The structural properties of a block of composite material composed of two plies have been produced. This example was designed to show the effect of ply angles in simple geometry (shown in Fig. 4) The lower block of material is unidirectional composite, whereas the top block has a variation in ply angle. The analysis centre is at the bottom left hand corner of the section. The material properties are shown in Table 3.

The angle of the fibres in the top block of material was varied from 0° (aligned with the lower block) through to 90°. Figure 5 shows the variation of elastic and shear centres with ply angle. The shear centre and elastic centre are, as expected, 5mm up from the bottom of the section when the ply angle is 0°. The elastic centre

Table 2
Shear stiffness accuracy with increase in linear elements through cross-section

Number of elements	Difference
4	+11·6%
10	+4·7%
20	+2·4%
40	+1·2%
80	+0·5%
160	+0·3%

https://doi.org/10.1017/S0001924000000105 Published online by Cambridge University Press

$$\mathbf{S} = \begin{pmatrix} 1{\cdot}7857\times10^{-8} & 0 & 0 & 0 & 0 & 0 \\ 0 & 5{\cdot}5029\times10^{-8} & 0 & 0 & 0 & 0 \\ 0 & 0 & 5{\cdot}4368\times10^{-8} & 0 & 0 & 0 \\ 0 & 0 & 0 & 5{\cdot}0708\times10^{-10} & 0 & 0 \\ 0 & 0 & 0 & 0 & 5{\cdot}3571\times10^{-10} & 0 \\ 0 & 0 & 0 & 0 & 0 & 1{\cdot}3393\times10^{-10} \end{pmatrix} \quad \ldots (27)$$

$$\mathbf{K} = \begin{pmatrix} 5{\cdot}600\times10^{7} & 0 & 0 & 0 & 0 & 0 \\ 0 & 1{\cdot}8172\times10^{7} & 0 & 0 & 0 & 0 \\ 0 & 0 & 1{\cdot}8393\times10^{7} & 0 & 0 & 0 \\ 0 & 0 & 0 & 1{\cdot}9721\times10^{9} & 0 & 0 \\ 0 & 0 & 0 & 0 & 1{\cdot}8667\times10^{9} & 0 \\ 0 & 0 & 0 & 0 & 0 & 7{\cdot}4667\times10^{9} \end{pmatrix} \quad \ldots (28)$$

moves into the lower block of plies as the angle of the upper block is changed. This is as would be expected because the axial stiffness of the upper block is reducing in comparison with the lower block. The trend for the shear centre is for the centre of twist to move into the upper block as the shear stiffness of the carbon fibre material is higher along the fibre than across it. The peak at around 40° is due to shear-extension coupling. The shear stiffness of the upper block material is effectively larger as the block wants to extend when sheared, and is restrained by the lower block.

The structural properties also vary with ply angle (see Fig. 6). The axial stiffness (labelled *EA*) is calculated at the elastic centre and decreases as the ply angle is changed from 0° to 90°. This, along with the bending stiffness variation (EI_{YY}), is an accordance with the reduction in axial stiffness of the upper block of material with angle.

4.3 NORMAL MODE RESPONSE OF COMPOSITE BOX-SECTION

A relatively simple rectangular section (Fig. 7) was chosen for linear normal mode analysis. The material properties are shown in Table 4.

The example is that of a simple untwisted composite box-section of length 1,000mm. Two finite element models were required to compare the normal modes analyses. The first, using shells and solids with the material properties defined in Table 4 as the benchmark. The second, made from beams using properties based on analysis of the cross-section using the method described within this work (Table 5). The mass properties were calculated by integrating all of the density, element cross-section area and centroid location terms in accordance with standard theory e.g. Young[2].

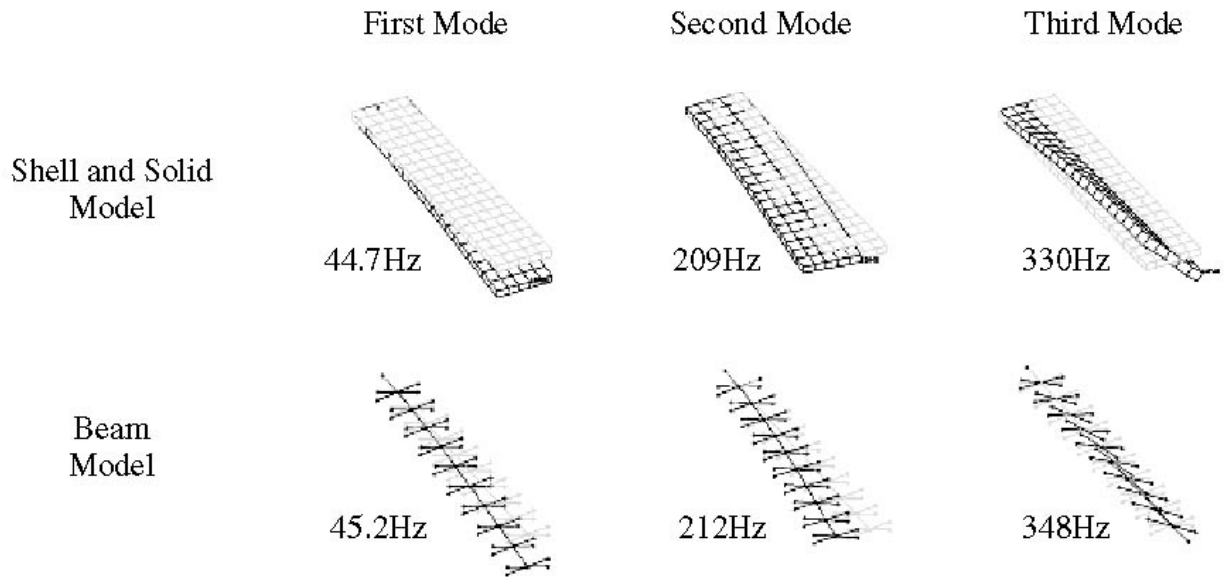


Figure 8. Normal mode response of shell and beam models.

https://doi.org/10.1017/S0001924000000105 Published online by Cambridge University Press

Table 3
Composite material properties

Property	Value
E_{11}(MPa)	131,500
E_{22}(MPa)	9,200
E_{33}(MPa)	9,200
G_{102}(MPa)	4,875
G_{13}(MPa)	4,875
G_{23}(MPa)	3,100
ν_{12}	0·3
ν_{13}	0·3
ν_{23}	0·45

Table 4
Material properties for normal mode example models

Material Property	Carbon/Epoxy	Generic Foam
E_{11}(MPa)	131,500	70
E_{22}(MPa)	9,200	70
E_{33}(MPa)	9,200	70
G_{12}(MPa)	4,875	25
G_{13}(MPa)	4,875	25
G_{23}(MPa)	3,100	25
ν_{12}	0·3	0·4
ν_{13}	0·3	0·4
ν_{23}	0·45	0·4
Density(kg/m^3)	1,600	50

Table 5
Required section properties for beam elements

Structural property	Value	Mass property	Value
EA(N)	$1{\cdot}203 \times 10^8$	Area (m^2)	0·006
EI_{YY}(Nm^2)	$1{\cdot}787 \times 10^4$	Mass/unit length (kgm^4/m)	2·921
EI_{ZZ}(Nm^2)	$3{\cdot}988 \times 10^5$	Mass Moment (I_{YY}) (kgm^4/m)	0·0054
GJ(Nm^2)	$2{\cdot}018 \times 10^4$	Mass Moment (I_{ZZ}) (kgm^4/m)	0·127
k_YGA(N)	$2{\cdot}611 \times 10^7$	Torsional Mass Moment (J) (kgm^4/m)	0·1326
k_ZGA(N)	$1{\cdot}172 \times 10^6$		

Table 6
Section and material properties assigned to beam model elements

Section property	Value	Material property	Value
A (m^2)	0·006	E (N/m^2)	$2{\cdot}01 \times 10^{10}$
I_{YY} (m^4)	$8{\cdot}95 \times 10^7$	G (N/m^2)	$7{\cdot}69 \times 10^9$
I_{ZZ} (m^4)	$2{\cdot}00 \times 10^5$	Density (kg/m^3)	≈ 0
J (m^4)	$2{\cdot}63 \times 10^6$		
k_Y	0·56		
k_Z	0·02		

Whilst modelling a prismatic composite structure using a 1D general beam section with an isotropic material, it is not usually possible to meet all of the mass and stiffness terms to the desired accuracy. This is due to the difference in I_{YY} and I_{ZZ} requirements between the overall mass and stiffness properties. It is therefore advised that the stiffness properties are calculated exactly, and the inertia terms simulated by putting point-masses on stiff beams. This should give rise to good correlation between shell and beam models of the natural modes of the structure. This is sufficiently accurate because the critical mass and stiffness terms of the models are virtually identical.

The properties used in the beam model analysis are shown in Table 6. In terms of the overall mass and structural properties of the beams, all are well within 1% of the values calculated. As each structural beam element was 100mm long, the total mass at each section along the beam needed to be 0·292kg. The mass and inertia properties were achieved by using 4 point masses, each of 0·073kg, placed 66mm horizontally and 13·6mm vertically away from the beam elements. It should be noted that it is necessary to halve the mass value for the tip node to obtain a consistent mass distribution along the model.

The normal mode results for the shell and beam models are shown in Fig. 8. The frequencies compare well with each other for each of the three modes, with the largest discrepancy being less than 6%. The beam model tends to be slightly stiffer, especially in torsion, which is due to the beam formulation not accounting for the cross-section deformation which can be seen in the shell and solid model.

5.0 CONCLUSIONS

A system for calculating structural properties of arbitrary beam sections with varying material properties has been developed. It calculates a fully populated 6×6 stiffness matrix for an equivalent 1D beam. It uses standard finite element software (PATRAN and NASTRAN) to analyse a thin 3D slice of the beam section. The stiffness values calculated compare well with theory available for simple isotropic beams, and so give confidence that the method can be applied to more complex structures.

ACKNOWLEDGEMENTS

Acknowledgements are made to EPSRC for providing funding under contract GR/N20898/01. Special gratitude is reserved for Pete Wood and Dave Swabey of AgustaWestland for their continued support and advice.

REFERENCES

1. MANSFIELD, E.H. and SOBEY A.J. The fibre composite helicopter blade, *Aeronaut Q*, May 1979, pp 413-417.
2. YOUNG, W.C. *Roark's Formulas for Stress Strain*, 1989, **6**, McGraw-Hill.
3. MANSFIELD, E.H. The stiffness of a two-cell anisotropic tube, *Aeronaut Q*, 1981, pp 338-353.
4. BARTHOLOMEW, P. and MERCER, A.D. Analysis of an anisotropic beam with arbitrary cross-section, RAE TR-84058, 1984, Farnborough, UK.
5. WÖRNDLE, R. Calculation of the cross-section properties and the shear stress of composite rotor blades, *Vertica*, 1982, **6**, pp 111-129.
6. GIAVOTTO, V., BORRI, M, MANTEGAZZA, P. and GHIRINGELLI, G. Anisotropic beam theory and applications, *Computers and Structures*, 1983, **16**, (1-4), pp 403-413.
7. KOSMATKA, J.B. and FRIEDMANN, P.P. Vibration analysis of composite turbopropellers using a nonlinear beam-type finite element approach, *AIAA J*, 1989, **27**, (11).
8. KOSMATKA, J.B. and DONG, S.B. Saint-Venant solutions for prismatic anisotropic beams, *Int J Solids Structures*, 1991, **28**, (7), pp 917-938.

https://doi.org/10.1017/S0001924000000105 Published online by Cambridge University Press

9. KOSMATKA, J.B. General behaviour and shear centre location of prismatic anisotropic beams via power series, *Int J Solids Structures*, 1994, **31**, (3), pp 417-439.
10. KOSMATKA, J.B. and DONG, S.B. General behaviour and shear centre location of advanced composite beams via power series, Proc AIAA/ASME/ASCE/AHS structural Dynamics and Materials Conference, 1996, 3, pp 1431-1439.
11. LEKHNITSKII, S.G. Theory of elasticity of an anisotropic elastic body., 1963, Translated by FERN, P. Holden-Day, San Francisco.
12. HODGES, D.H. Review of composite rotor blade modelling, *AIAA J*, 1990, **28**, (3), pp 561-565.
13. JOHNSON, E.R., VASILEV, V.V and VASILEV, D.V. Anisotropic thin-walled beams with closed cross-sectional contours, *AIAA J*, 2001, **39**, (12), pp 2389-2393.
14. CESNIK, C.E.S. and SHIN, S. On the modeling of integrally activated helicopter blades, *Int J Solids and Structures*, 2001, **38**, pp 1765-1789.
15. CESNIK , C.E.S., HODGES and D.H. VABS. A new concept for composite rotor cross-sectional blade modeling, *J American Helicopter Soc*, 1997, **42**, (1), pp 27-38.
16. PAIK, J., VOLOVOI, V. and HODGES, D.H. Cross-sectional sizing and optimization of composite rotor blades, 2002 AIAA Paper 2002-1322, Proceedings of the 43rd AIAA/ASME/ASCE/AHS/ASC Structures, Dynamics and Materials Conference, Denver, Co, USA.
17. BULL, J.W. (Ed), *Numerical Analysis and Modelling of Composite Materials*, Chapter 1, analysis of composite rotor blades, 1995, Chapman and Hall.
18. RAND, O. Fundamental closed-form solutions for solid and thin-walled composite beams including a complete out-of-plane warping model, *Int J Solid Struct*, 1998, **35**, (21), pp 2775-93.
19. ALKAHE, J. and RAND, O. Analytic extraction of the elastic coupling mechanisms in composite blades, *Composite Structures*, 2000, **49**, pp 399-413.
20. RAND, O. On the importance of cross-sectional warping in solid composite beams, *Composite Structures*, **49**, pp 393-397.
21. BAUCHAU, O. A beam theory for anisotropic materials, *J Appl Mech*, 1985, 52, pp 4126-422.
22. CHATTAPADHYAY, A., ZHANG, S. and JHA, R. Structural and aeroelastic analysis of composite wing box sections using higher-order laminate theory, Proc AIAA/ASME/ASCE/AHS Structural Dynamics and Materials Conference, 1996, **3**, pp 2185-2198.
23. CHANDRA, R., STEMPLE, A.D. and CHOPRA, I. Thin-walled composite beams under bending, torsional and extensional loads, *J Aircr*, 1990, **27**, (7), pp 619-626.
24. CHANDRA, R. and CHOPRA, I. Structural behaviour of two-cell composite rotor blades with elastic couplings, *AIAA J*, 1992, **30**, (12), pp 2914-2921.
25. HILL, G.F.J. and WEAVER, P.M. Analysis of arbitrary beam sections with non-homogeneous anisotropic material properties, Proc of the 13th International Conference on Composite Materials, ICCM13, June 2001 Beijing.
26. HILL, G.F.J. and WEAVER, P.M. Structural properties of helicopter rotor blade sections, Paper 55, Proc of the 28th European Rotorcraft Forum, September 2002, Bristol, UK.
27. MSC PATRAN 2001, MacNeal-Schwendler Corporation, 2975 Redhill Avenue, Costa Mesa, California 92626, USA.
28. MSC NASTRAN Version 70.7, MacNeal-Schwendler Corporation, 2975 Redhill Avenue, Costa Mesa, California 92626, USA.
29. GERE, J.M. and TIMOSHENKO, S.P. Mechanics of Materials, 1997, 4th Ed., London PWS, Boston, USA.

https://doi.org/10.1017/S0001924000000105 Published online by Cambridge University Press